Ordered oxide layers on the pentagonal surface of AlPdMn quasicrystal

S. Burkardt[1] and M. Erbudak[1,2]
[1]*Laboratorium für Festkörperphysik, ETH Zurich, CH-8093 Zurich, Switzerland*
[2]*Boğaziçi University, 34342 Bebek, TR-Istanbul, Turkey*
(Received 13 July 2009; revised manuscript received 23 September 2009; published 12 February 2010)

Recently, we reported the structural investigation of the oxide layers grown on the pentagonal surface of icosahedral $Al_{70}Pd_{20}Mn_{10}$ quasicrystal based on low-energy electron diffraction. The oxide layer was described to consist of five twin domains rotated by $2\pi/5$ with respect to each other in accordance with the symmetry of the quasicrystalline substrate each of which having one twofold-symmetry direction of the substrate as a mirror plane. Here, we discuss the oxidation process in more detail and report the growth of different oxide structures depending on the sample temperature and its pretreatment. At room temperature, amorphous oxide layers form. In contrast five distinct and few-nanometer-large domains possessing an internal hexagonal structure with substantial amount of contribution from antiphase domain boundaries grow at 700–800 K for small and large coverage. In an intermediate range, a mixture of antiphase domain-boundary contributions and fractional-order spots characteristic to a $2\sqrt{3}(1\times1)R\pm30°$ reconstruction of the surface oxide layer is found which additionally stabilized the interface. The previously reported twin-domain model, which was derived after an ion bombardment of the preoxidized surface with subsequent reoxidation, is identified as an oxide layer grown on the (110) surface of a crystalline $Al_{50}(PdMn)_{50}$ alloy as a result of the sputtering.

DOI: 10.1103/PhysRevB.81.085417 PACS number(s): 61.44.Br, 61.46.Hk, 61.05.J−, 68.47.Gh

I. INTRODUCTION

Ordered oxide films on metal substrates have gained considerable interest because of their attractive properties as carriers for metal catalysts and their applications in communication industry.[1] By virtue of their excellent thermal, chemical, and mechanical stability, they are also used as surface capping to protect the bulk material against wear and corrosion. It is a practical advantage that due to the shallow structure of the oxide films no charge accumulation takes place and the oxide characterization can be performed with ease.

The investigations of the epitaxially grown oxide films[2–4] reveal several common features: the surface layer is ionic and has a thickness in the subnanometer range. Quite frequently, the extent of commensurability of the overlayer with the substrate structure produces Moiré patterns that render the interpretation of the real-space structure difficult. The structural analysis of the film using low-energy electron diffraction (LEED) is very convenient owing to the averaging properties of the method, yet it presents a serious challenge since the film thickness is comparable with the mean-free path of the electrons leading to multiple scattering involving the interface. Al-oxide films that form a distorted hexagonal lattice on Ta(110),[2] FeO(111) grown on Pt(111) (Ref. 3) as well as on Ru(0001) (Ref. 4) surfaces are interesting examples.

The formation of oxide layers on Al metal has been studied intensively. The properties of the surface films depend on the crystal face of Al and the surface preparation. While ordered layers of dissociative chemisorbed oxygen are routinely achieved even at elevated temperatures,[5] the quality of the structure of the oxide film requires some care in preparation. At low temperatures, an Al-deficient amorphous oxide film grows that prevents inward diffusion of O and outward diffusion of Al. At high temperatures, an Al-rich amorphous oxide layer forms on Al metal which crystallizes upon heat treatment. Ordered binary Al-transition-metal (TM) alloys have been studied also fairly extensively.[6–11] On NiAl(110), large[12] and ordered Al-oxide domains are formed with an internal structure resembling the (111) surface of θ or the (001) surface of κ-Al_2O_3. The domains are partly commensurate with the substrate, about 0.5 nm thick, and oxygen terminated. Consistent with the orthogonal symmetry of the NiAl(110) surface, two equal domains form with the $[1\bar{1}0]$ direction of the surface being the mirror axis.[7] The slight distortion of the topmost NiAl layer upon oxidation[10] and the resulting complex structure of the interface[11] have made the structure determination of the oxide film complicated. The LEED pattern and the scanning tunneling microscopy (STM) images are dominated by the antiphase ordering of the reflection domains[8,9] while the quasihexagonal pattern of the Al-oxide structure is still discernible.

Quasicrystals, especially the ternary compounds based on Al, resemble structurally and electronically Al-TM binary alloys, except that they possess long-range orientational and quasiperiodic translational order.[13] $Al_{70}Pd_{20}Mn_{10}$ (AlPdMn) has a structure which has icosahedral (*i*) symmetry with atomically dense planes perpendicular to the fivefold-symmetry directions.[14] Depending on the sample preparation, the pentagonal surface can consist of micron-large flat terraces[15,16] and therefore is an ideal substrate for the growth of thin oxide films. Recently, it has been reported that a well-ordered Al-oxide layer forms on the pentagonal surface of *i*-AlPdMn quasicrystal as a result of oxygen exposure at 700 K.[17] LEED patterns have been used to extract real-space information about the surface oxide structure. The presence of multiple domain orientations complicates the identification of the surface structure of each individual domain considerably. An elegant way to surmount this problem was to sputter the oxidized surface briefly with Ar^+ ions at grazing incidence in order to have one domain orientation to survive the ion bombardment. Finally, the domain structure was described to consist of five twin domains each of which having one twofold-symmetry direction of the substrate as a mirror

plane from which the components of the twin are rotated away by $\pm 23.25°$. Each twin domain is then rotated by $2\pi/5$ with respect to the others in accordance with the rotational symmetry of the substrate. The identification of the oxide domain structure was primarily based on the analogy between the *i* structure of AlPdMn and the CsCl structure of Al-TM alloys.

In the present work, we identify this oxide layer as a layer grown on the (110) surface of a crystalline $Al_{50}(PdMn)_{50}$ alloy that is generated as a result of Ar^+-ion bombardment. Additionally, we report two other oxide domain structures based on a hexagonal main lattice.

II. EXPERIMENTAL

We have used a sample with dimensions $9\times 8\times 1$ mm^3, which was mounted onto a resistive heater and introduced into an ultrahigh-vacuum system with a base pressure in the low 10^{-9} mbar region. The sample temperature was measured with a chromel-alumel thermocouple (*K*-type) pressed onto the sample surface. For the experiment, the sample surface was cleaned by cycles of sputtering with Ar^+ ions (1.5 keV, 5×10^{-7} A/mm^2) at room temperature and subsequent heat treatment at 700–800 K for 60 min. A three-grid, back view, display-type LEED system with a total opening angle of $89\pm 2°$ (Ref. 18) and operating at low microampere primary currents was used to analyze the sample. Thus, a momentum transfer of 2.88 ± 0.05 Å^{-1} could be detected from a square lattice for 64 eV electrons at normal incidence. Patterns are recorded using a 16-bit charge-coupled-device camera and shown after normalization by the response function of the display and recording system in order to eliminate spurious contributions to the image. All the experimental procedures were similar to those in previous reports.[17,19,20]

III. RESULTS AND DISCUSSION

A. LEED from the oxidized surface

Figure 1(a) shows a LEED pattern from the clean pentagonal surface of *i* AlPdMn recorded at 64 eV. We observe fivefold symmetry with fairly well-defined spot profiles. The pentagonal surface contains five twofold-symmetry axes, one of which is indicated by arrows and a line through the pattern. These axes are determined in a straightforward way by comparing the LEED pattern with secondary-electron images recorded under the same sample geometry, using thereby the fact that the latter give real-space information.[19,21] Figures 1(b)–1(d) report patterns after different oxygen exposures, i.e., 36, 126, and 144 langmuirs (L), respectively, where 1 L stands for 1.3×10^{-6} mbar s. Several features can be detected by visual inspection of the patterns: (i) oxygen adsorption at the surface produces 30 fairly strong spots that appear at a polar angle of $35.7\pm 1°$. (ii) The spots show polar, and to a larger extent, azimuthal smearing. (iii) Beside the 30 main diffraction spots, there are numerous minor spots with smaller intensity either distributed radially in concentric groups of $5n$, where n is an integer, evenly over the screen [Fig. 1(c)] or (iv) located on ringlike features accompanying the main diffraction spots, best observable in Fig. 1(d). (v)

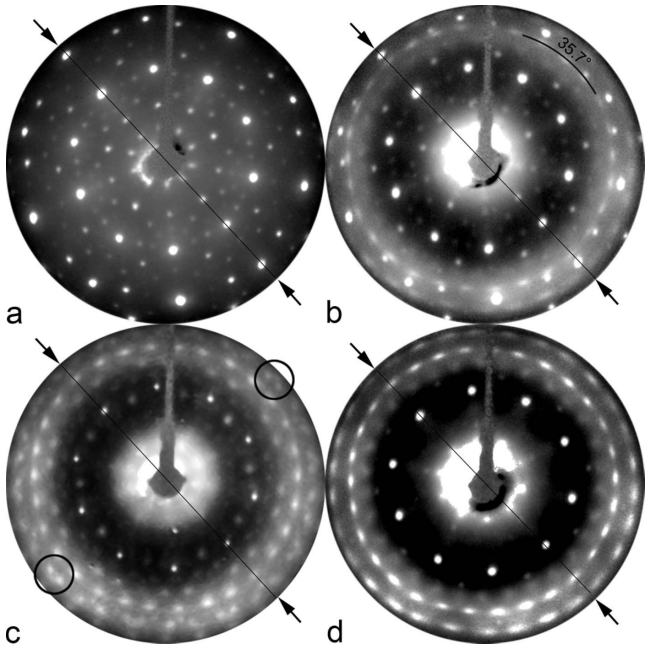

FIG. 1. LEED patterns at a primary-electron energy of 64 eV obtained from the (a) clean and [(b)–(d)] exposed pentagonal surface of *i* AlPdMn to 36, 126, and 144 L of oxygen at 740 K, respectively. One twofold-symmetry axis at the surface is indicated by a thin line and two arrows at the rim of the pattern. The encircled features are discussed in the text.

The diffraction spots originating from the oxide structure gradually appear and become sharper as the surface is exposed to more oxygen while only the intense spots from the quasicrystalline substrate are discernible at every stage of oxidation (but without any major change in spot profile). We note that due to the intensity saturation of the electron detector intense spots seem to have a large angular spread. (vi) These observations apply to more or less all the oxidized surfaces shown in Figs. 1(b)–1(d). In the following, we draw conclusions about the global and local structural properties of the oxide film and its interface with the quasicrystal.

The common characteristics of the patterns are 30 diffraction spots that already appear at the early stage of oxidation. This arrangement of spots has been encountered for epitaxial films that crystallize in sixfold-symmetric textures on the pentagonal surface of *i*-AlPdMn quasicrystal.[15,22] It represents a hexagonal domain structure that is repeated five times in equal azimuthal increments of $2\pi/5$. In the present case, chemical analysis of the film confirms that Al binds to oxygen while Pd and Mn remain unaffected by the exposure.[17] The polar radius of $35.7\pm 1°$ corresponds to an interatomic distance of $d=3.0\pm 0.06$ Å in a hexagonal mesh and reflects the distance of oxygen atoms in the Al-oxide film, which is expanded by 4–5 % relative to the Al_2O_3 bulk lattice constant.[7] The spots show an angular (polar) distribution which is compatible with a domain size of 30 ± 5 Å.[23] We note that there is a well-defined orientational relationship between the oxide and the substrate, i.e., the diffraction spots due to the oxide layer are aligned with the twofold-symmetry axes of the pentagonal surface.

In all the patterns shown in Fig. 1 the diffraction spots originating from the quasicrystal are distinctly observable

indicating that the oxide film is relatively thin. In the earlier work, the thickness was estimated to be 5 Å (Ref. 17) similar to the oxide films grown on the ordered Al-TM alloys.[6–11] For the film at low oxygen exposure [Fig. 1(b)] the diffraction pattern due to the quasicrystalline surface is not modified signaling that the quasicrystalline structure is preserved at the interface. Consequently, there is no intermediate layer between the quasicrystalline substrate and the crystalline oxide layer.[24] This statement cannot be substantiated for the oxide films shown in Figs. 1(c) and 1(d), as discussed later. We also note that within our capabilities, we cannot draw any firm conclusion about the growth mode of the oxide layer. However, the fact that the faint spots are not discernible for thicker oxide layers implies that the diminishing intensity is due to the oxide layer thickness (layer-by-layer growth, exponential decay) rather than a change in area, which is not covered by the oxide (island growth, linear decay), therefore, suggesting the growth of a closed oxide layer.[25,26]

The pattern in Fig. 1(b) mainly consists of a fivefold repetition of a hexagonal oxygen lattice. This diffraction characteristics is also found in Fig. 1(d), which shows a pattern from a surface with a thicker oxide layer. Additionally, a diffraction feature accompanies the main hexagonal spots which is similar to the satellite spots encountered in antiphase domain-boundary structured surface films.[2–4] The pattern shown in Fig. 1(c), on the other hand, displays additional minor spots evenly distributed over the screen signaling a surface reconstruction of the hexagonal domain structure. We note that some diffraction patterns show an uneven distribution of intensity in the main and/or the satellite spots signaling a preferential occupation of the five otherwise equally probable domain orientations.

B. Atomic structure of the domains

1. Antiphase domain boundaries

The patterns shown in Figs. 1(b) and 1(d) have in common that the main diffraction feature can be assigned to a fivefold repetition of a hexagonal mesh with some satellite spots arising from antiphase domain boundaries. The 30 main spots correspond to five hexagonal meshes, each placed in equal azimuthal increments of $2\pi/5$ with respect to the others, with an interatomic distance of approximately 3 Å. In order to account for the satellite spots, a real-space model is presented in Fig. 2(a). An idealized alignment of the domains on the surface gives rise to additional hexagonal diffraction spots oriented along the [11] direction accompanying the main spots. For the formation of the oxide domains, there are 5 degrees of freedom for the rotational alignment on the pentagonal surface of the *i* quasicrystal. Consequently, five groups of domains are required on the surface with equal probability, each rotated by $2\pi/5$ with respect to the others. Hence, the resulting diffraction pattern is generated by adding the contributions of the single domain characteristics, as shown in Fig. 2(b), to a composite diffraction pattern, as illustrated in Fig. 2(c).

The as-generated pattern reproduces satisfactorily the spots of the observed diffraction pattern shown in Fig. 2(d).

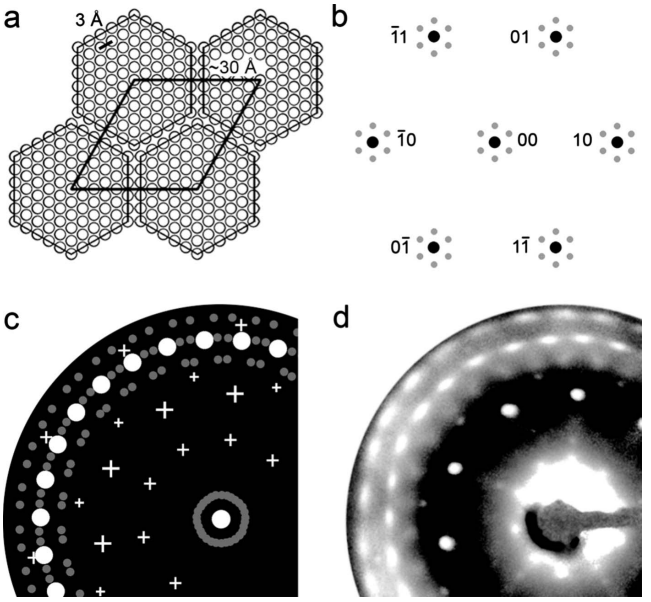

FIG. 2. (a) A real-space arrangement of four hexagonal domains. The interatomic distance and the domain size are approximately 3 and 30 Å, as deduced from the LEED pattern. (b) The reciprocal-space image of a single oxide domain configuration. The main spots drawn bold correspond to the hexagonal structure within the domain. (c) The diffraction pattern is superposed five times in equal azimuthal increments in order to mimic the observed diffraction pattern. Spots due to the quasicrystalline substrate are indicated as crosses. (d) For comparison an experimental LEED pattern.

The antiphase components along the [11] direction of the hexagonal structure is close to $\frac{1}{9}$ of the reciprocal-lattice vector. Thus, the real-space domain-boundary distances are approximately 28 Å, which can be well reproduced by the idealized arrangement of the domains. We note that this arrangement is the simplest interpretation of the LEED patterns. Most likely, there are further antiphase domain boundary contributions delivered in the LEED patterns, indicated by the bright centers of the patterns. A more complex ordering is observed by the oxidation of the 10*f*-symmetry surface of *d*-AlCoNi quasicrystal.[24] In the present case, the inferior quality of the patterns, which is most likely a consequence of the different oxide preparation condition,[12] hampers any firm conclusion about the exact ordering of the hexagonal domains on the surface. Nevertheless, the patterns confirm the growth of an antiphase domain ordering.

2. Surface reconstruction

The initial stage of the surface oxidation presented in Fig. 1(b) shows faint diffraction features indicating the presence and the interaction of the domain walls while most of the quasicrystal details remain discernible. On the surface shown in Fig. 1(d), on the other hand, almost all of the minor quasicrystal spots are concealed and the features due to the antiphase domain boundaries dominate the pattern. A further oxide structure is shown in Fig. 1(c). Its diffraction characteristics indicates a reconstruction of the surface layer but it is conceivable that the pattern also shows simultaneously

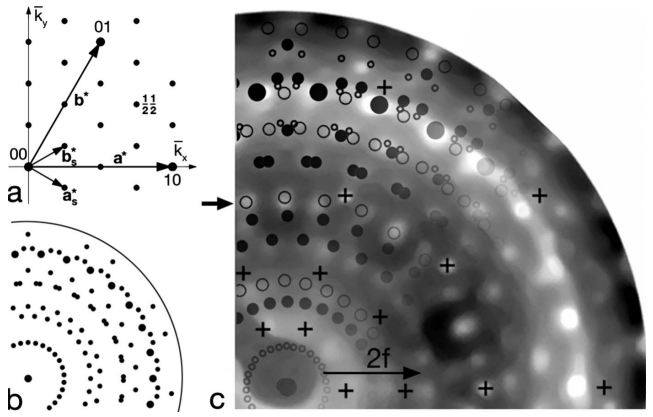

FIG. 3. (a) A reciprocal-space representation of the contribution of one oxide domain in hexagonal structure. The main spots with the unit vectors $\boldsymbol{a}^*$ and $\boldsymbol{b}^*$ are drawn bold compared to the minor spots due to the reconstruction. $\boldsymbol{a}_s^*$ and $\boldsymbol{b}_s^*$ are the unit vectors of the reconstruction. (b) Schematic pattern obtained by superposing the signal from each domain five times in equal azimuthal increments in order to mimic the observed diffraction spots. (c) For comparison a LEED pattern at an intermediate stage of oxidation is shown where some quasicrystalline spots are highlighted with crosses. A twofold-symmetry axis coincides with the horizontal.

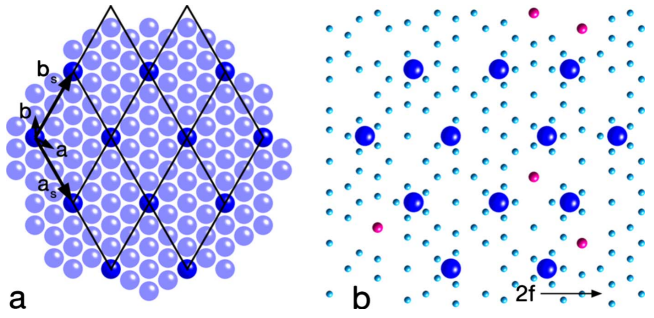

FIG. 4. (Color online) (a) One of the five surface oxide domains in real space which is about 30 Å large. The termination of oxygen atoms form a hexagonal mesh with the basis vectors $\boldsymbol{a}$ and $\boldsymbol{b}$ while the superstructure with the basis vectors $\boldsymbol{a}_s$ and $\boldsymbol{b}_s$ is 12 times larger than the hexagonal unit mesh. (b) The interface between the pentagonal surface of AlPdMn quasicrystal and oxygen atoms of an oxide layer. The quasicrystal surface is represented by computed coordinates (Ref. 14) with Al (small) and Mn (large) atoms while for the oxygen mesh only the superstructure atoms are drawn (largest) for clarity. The twofold-symmetry direction of the substrate is also indicated. The domain size is approximately 30 Å.

contributions from antiphase domain boundaries as well as contributions from a crystalline buffer layer.

The spots arising from the reconstruction can be identified by the formation of 30 concentric spots of equal azimuthal increments and intensity. In contrast, the additional spots due to the antiphase domain boundaries show often an uneven distribution of intensity consisting of double pairs of spots being rotated in equal azimuthal increments with respect to each other of the same brightness while the spots in between are fainter. This is comprehensible considering the averaging nature of the LEED experiment: while the intensity distribution of the antiphase domain diffraction characteristics sensitively depends on the orientation of the neighboring domains, that for the surface reconstruction does not.

In order to reproduce the contribution due to the reconstruction, we have tried several different surface-atom arrangements. Figure 3(a) presents the most-likely atomic structure in reciprocal space. The integer-order spots, drawn bold, originate from the hexagonal mesh of the surface oxide layer with the basis vectors $\boldsymbol{a}^*$ and $\boldsymbol{b}^*$. The basis vectors $\boldsymbol{a}_s^*$ and $\boldsymbol{b}_s^*$ of the surface unit mesh correspond to a $2\sqrt{3}(1\times1)R\pm30°$ reconstruction. In matrix notation, it can be expressed as $\frac{1}{6}\left(\begin{smallmatrix}2 & -1\\ 1 & 1\end{smallmatrix}\right)$ in reciprocal space. Since there are five distinct domains on the surface, each contributing equally to the observed pattern, five individual reconstructions are superimposed in order to mimic the diffraction pattern. This composite pattern is shown in Fig. 3(b).

For comparison, a LEED pattern from the oxidized pentagonal surface similar to that shown for 126 L of oxygen exposure, is presented in Fig. 3(c). A favorable comparison of the generated and recorded patterns is achieved by aligning a twofold-symmetry axis of the pentagonal surface with the direction $(\boldsymbol{a}_s^*+\boldsymbol{b}_s^*)$ of the surface reconstruction. The agreeable comparison makes us assume that this structure to be the most probable one. However, we note that it was not possible to reproduce all the diffraction spots observed in Fig. 3(c). The diffraction characteristics from the reconstruction and the antiphase domain boundaries are illustrated with the black dots as well as the small empty circles. There are some diffraction spots, one set is indicated by the black arrow, which are not covered by the surface structures so far. A further antiphase domain-boundary component, illustrated by the large empty circles, is suggested but the spots may also arise from the crystalline buffer layer, as discussed in the next section. Any firm conclusion is also obstructed regarding that the film thickness is in the same order of magnitude as the mean-free path of the electrons used in LEED. Thus, multiple-scattering effects involving the substrate are expected to contribute to the observed pattern and possibly are responsible for the features not accounted for by single scattering at the oxide layer.

Figure 4(a) reports a hexagonal structure for the oxygen-terminated oxide layer in real space with the unit vectors $\boldsymbol{a}$ and $\boldsymbol{b}$. Oxygen atoms form a domain as large as 30 Å in diameter with the interatomic distance of approximately 3 Å, as deduced from the LEED patterns. The superstructure is a hexagonal mesh, which is obtained by Fourier transforming the schematic pattern shown in Fig. 3(a). It is evident that the surface reconstruction can be represented in real space by the basis vectors $\boldsymbol{a}_s$ and $\boldsymbol{b}_s$ and the matrix $2\left(\begin{smallmatrix}1 & -1\\ 1 & 2\end{smallmatrix}\right)$, which is abbreviated as $(111)2\sqrt{3}(1\times1)R\pm30°$. Each reconstructed surface unit cell has an area of $6\sqrt{3}d^2$, where d represents the average interatomic distance and is thus 12 times larger than the unreconstructed cell of $\sqrt{3}/2d^2$ expected from the bulk-terminated (111) surface and, therefore, sufficiently large to produce its own diffraction pattern. This is the simplest model for the reconstruction where oxygen atoms are placed on a perfect hexagonal mesh and the resulting reconstructed cell is also hexagonal. More precise experimental findings with different methods will certainly refine this idealized model.

In an attempt to understand the formation of the large unit cell of the surface reconstruction, a comparison in real space of the reconstructed oxygen layer with the atom distribution at the pentagonal surface of *i* AlPdMn is shown in Fig. 4(b). This procedure gives very good results in reciprocal space[27] and is shown also to be promising for real-space data analysis.[22] The quasicrystal is represented by an Al-rich layer with some Mn atoms present.[14] In order to search for possible mechanisms that cause the reconstruction, an approximately 30 Å large domain was superimposed onto the quasicrystal surface. For clarity, the oxygen atoms other than those at the corners of the reconstructed cells are omitted. Additionally, some displacement of these corner atoms have been allowed. In the Fig. 4(b), it is evident that there is a considerable registry between the aperiodic and the crystalline structures over the entire domain. We recall that the LEED spots show a certain relaxation in the azimuthal direction. This relaxation provides an additional stabilization of the crystalline domains on the quasicrystal surface. A similar adsorbate constellation with azimuthal relaxation has been encountered for the chemisorption of oxygen on the tenfold-symmetry surface of *d*-AlCoNi quasicrystal.[20,28]

The reconstructed surface unit cell is spanned by two basis vectors $\boldsymbol{a}_s$ and $\boldsymbol{b}_s$. Only the alignment of the atomic rows along $(\boldsymbol{a}_s+\boldsymbol{b}_s)$, or perpendicular to $\boldsymbol{b}$, parallel to a twofold-symmetry direction of the substrate, as shown in Fig. 4(b), results in a satisfactory registry with the substrate. The registry results by virtue of the overlap of the reconstructed surface with the atomic positions of the quasicrystal surface, which we take as the driving force for this *supercell epitaxy*. The exact registry of the Al-oxide islands on *i* AlPdMn is observed in reciprocal space, i.e., in the LEED patterns and, additionally, found in the real-space model considerations. Thus, for the alignments of the domains in a way shown both in reciprocal and real space, illustrated in Figs. 3 and 4, respectively, the mismatch between the crystalline and quasicrystalline lattice goes through an energy minimum. Consequently, the result is an interface, which has a high degree of structural registry and, together with the azimuthal degree of freedom by a few degrees, could explain the stabilization of the crystalline oxide islands at the quasicrystal surface.

3. Crystalline buffer layers

Al deficiency at the surface of the AlPdMn alloy was reported to shift the quasicrystalline equilibrium toward the CsCl structure.[29] The quasicrystalline ordering is restored as soon as Al is replenished by diffusion from the bulk to the surface as a result of heat treatment. In the present case, Al atoms bind to oxygen and will be absent in the alloy. This may similarly shift the alloy stoichiometry toward the binary alloy and destroy the quasicrystalline ordering. But, since the oxidation is performed at elevated temperatures, Al diffusion is effective in the bulk quasicrystal and an Al-oxide film forms without adversely modifying the quasicrystalline stoichiometry and structure of the surface. Hence, there is a balance between the diffusion of Al to the surface[22] and the rate of oxidation for a particular temperature and oxygen dose.[30]

The formation of a buffer layer on the quasicrystal surface in the CsCl structure can still be induced by the conditions during oxidation, e.g., a lower sample temperature that hinders sufficient Al replenishment from the bulk. Alternatively, a buffer layer can be formed by Ar^+-ion bombardment that reduces the Al concentration in the alloy and shifts the structural stability toward the cubic crystal.[31] While in the first case the buffer layer is expected to be extremely thin due to the shallowness of the oxide layer, the impact of the ion bombardment on the surface is rather drastic.[32] In an earlier attempt to characterize the oxide structure on the pentagonal surface,[17] brief sputtering of the oxidized surface and subsequent high-temperature reoxidation was used to identify one single domain out of the five equally probable multiple domains on the surface. As communicated elsewhere,[33] we claim that this oxide structure is identical to the oxide layers grown on binary Al-TM alloys.[16,11]

Previous studies with thin Gd_2O_3 layers have shown that the range of impact of Ar^+ ions is in the order of magnitude larger than the Al-oxide layer thickness.[32] Therefore, it is not surprising that an oxide layer is formed on the sputtered surface, which is characteristic to crystalline binary Al-TM oxides. The structure of these oxide layers can be summarized as a slightly distorted $6\times 2\sqrt{3}$ reconstruction.[17] The twinning is caused by the fact that the twofold-symmetry axes of the quasicrystal coincide with a mirror plane of the buffer layer in the CsCl structure.[29] The reproduction of the LEED pattern obtained from the Ar^+-ion bombarded surface using the twin model is very convincing [the reader is referred to Figs. 1c and 1d of Ref. 17]. Such patterns contain a characteristic feature in the form of pairs of double spots near the rim of the collector screen and outside the set of diffraction spots due to the hexagonal mesh. One pair is encircled in Fig. 1(c) and signals the presence of a buffer layer for this surface.

IV. CONCLUSIONS

Oxygen exposure at high temperatures results in a thin Al-oxide layer on the fivefold-symmetry surface of the Al-PdMn quasicrystal. With the aperiodic atomic order of the quasicrystalline template, the system finds the best compromise by breaking up into domains ordered in a hexagonal structure where each domain remains locally commensurate and in registry with the substrate. This registry leads to five distinct orientations with respect to the substrate while the small domain size is determined by a large interfacial strain energy. Beside this basic structural consideration, the registry of the Al-oxide islands with the aperiodic substrate structure is realized by the superstructure of the surface layer, i.e., the Al-oxide layer is reconstructed in order to lower the interfacial strain energy. This case can be considered as a typical epitaxy-stabilized reconstruction. The reconstruction is not observed for low and high coverage, which remains an unexplained observation. Instead, the electron-diffraction results signal the highly ordered interaction of the grain boundaries of the domains.

Crystalline surface oxides on quasicrystal surfaces provide chemical and mechanical protection of the bulk material. The natural growth mechanism of the oxide layer leads

to nanometric islands of a size that is interesting for quantum-well applications, catalyst carriers, or magnetic storage units. Technological applications, however, require a wider availability of quasicrystals for serious considerations. Here, we have presented electron-diffraction patterns from the oxidized quasicrystal surface. While a single diffraction pattern displays the surface structure averaged over a region related to the electron coherence zone, details of the surface morphology, such as roughness or defects, remain concealed. Only STM can investigate the precise surface domain structure. Therefore, the present work is to stimulate and encourage further investigations based on scanning probe techniques which would augment and complement our proposed oxide model.

ACKNOWLEDGMENTS

We are indebted to G. Kasner for the coordinates of the AlPdMn quasicrystal. Financial support was provided by the ETH Zurich and the Schweizerischer Nationalfonds.

[1] M. Schmid, G. Kresse, A. Buchsbaum, E. Napetschnig, S. Gritschneder, M. Reichling, and P. Varga, Phys. Rev. Lett. **99**, 196104 (2007).
[2] P. J. Chen and D. W. Goodman, Surf. Sci. **312**, L767 (1994).
[3] W. Ranke, M. Ritter, and W. Weiss, Phys. Rev. B **60**, 1527 (1999).
[4] G. Ketteler and W. Ranke, Phys. Rev. B **66**, 033405 (2002).
[5] J. Trost, H. Brune, J. Witterlin, R. J. Behm, and G. Ertl, J. Chem. Phys. **108**, 1740 (1998), and references therein.
[6] G. Kresse, M. Schmid, E. Napetschnig, M. Shishkin, L. Köhler, and P. Varga, Science **308**, 1440 (2005).
[7] R. M. Jaeger, H. Kuhlenbeck, H.-J. Freund, M. Wuttig, W. Hoffmann, R. Franchy, and H. Ibach, Surf. Sci. **259**, 235 (1991).
[8] G. Ceballos, Z. Song, J. I. Pascual, H.-P. Rust, H. Conrad, M. Bäumer, and H.-J. Freund, Chem. Phys. Lett. **359**, 41 (2002).
[9] M. Kulawik, N. Nilius, H.-P. Rust, and H.-J. Freund, Phys. Rev. Lett. **91**, 256101 (2003).
[10] E. W. A. Young and J. H. W. De Wit, Solid State Ionics **16**, 39 (1985).
[11] A. Stierle, F. Renner, R. Streitel, H. Dosch, W. Drube, and B. C. Cowie, Science **303**, 1652 (2004).
[12] The reconstructed surface unit cell is about 16 times larger than that of the bare substrate.
[13] *Physical Properties of Quasicrystals*, Springer Series in Solid-State Sciences, edited by Z. M. Stadnik (Springer, Berlin, 1999).
[14] Z. Papadopolos and G. Kasner, Phys. Rev. B **72**, 094206 (2005).
[15] H. R. Sharma, M. Shimoda, and A. P. Tsai, Adv. Phys. **56**, 403 (2007).
[16] B. Ünal, C. J. Jenks, and P. A. Thiel, Phys. Rev. B **77**, 195419 (2008).
[17] J.-N. Longchamp, S. Burkardt, M. Erbudak, and Y. Weisskopf, Phys. Rev. B **76**, 094203 (2007).
[18] Ociepa Microengineering, London, ON N5W 4R3, Canada.
[19] M. Erbudak, M. Hochstrasser, E. Wetli, and M. Zurkirch, Surf. Rev. Lett. **4**, 179 (1997).
[20] S. Burkardt, S. Deloudi, M. Erbudak, A. R. Kortan, M. Mungan, and W. Steurer, J. Phys.: Condens. Matter **20**, 314006 (2008).
[21] Y. Weisskopf, R. Lüscher, and M. Erbudak, Surf. Sci. **578**, 35 (2005).
[22] R. Lüscher, in *Surface Science: New Research*, edited by C. P. Norris (Nova Science, New York, 2005).
[23] M. Horn-von Hoegen, Z. Kristallogr. **214**, 591 (1999).
[24] S. Burkardt, M. Erbudak, and R. Mäder, Surf. Sci. **603**, 866 (2009).
[25] H. Lüth, *Solid Surfaces, Interfaces, and Thin Films* (Springer-Verlag, Berlin, 2001).
[26] The *d*-AlCoNi quasicrystal can be prepared and oxidized at much higher temperatures compared to the *i*-AlPdMn quasicrystal due to different melting temperatures, see, e.g., Ref. 15.
[27] E. J. Widjaja and L. D. Marks, J. Phys.: Condens. Matter **20**, 314003 (2008).
[28] M. Erbudak, M. Mungan, and S. Burkardt, Appl. Surf. Sci. **256**, 1284 (2009).
[29] B. Bolliger, M. Erbudak, D. D. Vvedensky, M. Zurkirch, and A. R. Kortan, Phys. Rev. Lett. **80**, 5369 (1998).
[30] H. Brune, J. Wintterlin, J. Trost, G. Ertl, J. Wiechers, and R. J. Behm, J. Chem. Phys. **99**, 2128 (1993).
[31] Y. Weisskopf, *Growth of CsCl-Type Domains on Icosahedral Quasicrystal Al-Pd-Mn* (Logos Verlag, Berlin, 2006).
[32] T. Flückiger, M. Erbudak, A. Hensch, Y. Weisskopf, M. Hong, and A. R. Kortan, Surf. Interface Anal. **34**, 441 (2002).
[33] J.-N. Longchamp, S. Burkardt, M. Erbudak, and Y. Weisskopf, Phys. Rev. B **80**, 149901(E) (2009).